
Chapter-6

Biocompatibility Behavior of Ta-Coated 316L Stainless Steel

6.0 Introduction

Surgical-grade stainless steel alloys are widely used to develop bio-implants such as screws, plates, nails, and hip joints due to their biocompatibility, high mechanical strength, and availability. About 70% of hip joints made in the USA are manufactured using 316L steel[198]. By 2022, the global medical device and implant market is estimated to exceed \$110 billion[199]. However, decades of study and biomedical observation have shown that several issues with surgical grade 316L SS still need to be resolved. Firstly, because of its low biocompatibility, the implants only form a weak chemical bond with the bones rather than a mechanically strong one. Secondly, because 316L SS has a high concentration of Ni (12 wt %) and Cr (17 wt %), pitting corrosion and releasing of nickel ions usually take place when implants come into contact with biological fluids[200]. Austenitic stainless steel, Co–Cr-based alloys, and titanium alloys are currently the most widely used biomedical metals for bone restoration applications. Because the Cr element may produce a stable passive surface oxide film to defend against corrosion attack, austenitic stainless steels are the most commonly chosen for artificial implants[201-202]. ASTM F138 and F139 specifications are used to confirm the chemical requirements for implant-quality stainless steel. Low phosphorus concentration provides better ductility, especially for surgical implants, to improve strength[203]. Compared to both polymers and ceramics, metallic biomaterials perform better in several ways. Due to its strong biocompatibility and osteointegration properties, tantalum is a significant metallic biomaterial frequently used in bone repair applications [204]. After the bone has healed, a metallic

implant must be removed during surgery. In adverse circumstances, tantalum's corrosion resistance is also more significant than titanium and stainless steel [205]. The ability of Ta implants to develop a self-passivating Ta₂O₅ surface coating with excellent stability over a broad potential-pH range is primarily responsible for their good corrosion resistance and biocompatibility. Additionally, Ta₂O₅ films, which have a robust insulating property, do not cause the protein to denature, which promotes early cell attachment and tissue ingrowth [206-207]. Ta-based biomaterials are considered suitable for prospective coating materials in biomedical applications because their use in bulk is restricted by both high density and cost. Ta₂O₅ films have been created using a variety of surface modification techniques, such as plasma ion implantation (PII), chemical vapor deposition, and physical vapor deposition approaches [208-209].

However, the resultant film thicknesses are generally less than 100 nm because of stagnation growth performance. This thus decreases the coated implants' long-term dependability[204]. A matrix must be biocompatible in order to allow adequate cellular activity, including the stimulation of molecular and mechanical signalling systems that promote tissue regeneration[210]. This means it should not induce any undesirable local or systemic interactions in the eventual host. Tantalum coatings enhanced cellular interactions and proliferation in biological assays using mesenchymal stem cells extracted from human bone marrow[211]. When the surface of 316L SS for coronary stents was modified to provide an anti-thrombogenic surface, the TaC_xN_{1x} coating can be a great candidate [209]. An inner tantalum layer and two outer layers of 316L stainless steel comprise the stent's trilayer composite metal structure. Major adverse cardiac events are rare in the first month; in this trial, which included individuals with lesions at substantially reduced risk, there was a 1.0% incidence. The first clinical implementation of tantalum, stainless steel, and PC-

coated triplex stent [212]. Concerning stainless steel substrates, the optimized Fe-based bulk metallic glass coating samples demonstrated lower cytotoxicity, improved cell adhesion, and higher blood compatibility[213]. The MG 63 osteoblast cells were strongly attracted to, dispersed out, and differentiated on the 316L SS, exhibiting improved biocompatibility as the concentration was enhanced of Ce in Nb₂O₅-coated 316L SS [214]. According to a recent study, rapid, uniaxial migration seen in febrile 3D cell-derived matrices can be mimicked in many ways by 1D topography, and both 1D and 3D migrations differ from 2D migration in terms of cell morphology, cytoskeleton structure, and function [215].

Over the past 20 years, various surface modification techniques have been created; it has been proven that changes in surface wettability, hydrophobicity, and surface charges affect how much protein adsorption occurs. Overall, it has been established that increasing surface hydrophilicity improves the biocompatibility of implantable implants in vitro[215]. Despite the extensive literature on promising in vitro outcomes, surface functions seem to have little success in significantly altering tissue responses in vivo [216]. Magnetron sputtering deposition has been widely recommended as an adaptable deposition technique with many benefits, including high deposition rates, ease of sputtering the preferred metal, alloy, or compound, formation of high-purity films, extremely high film adhesion, and the ability to form dense coatings[217-219]. However, a stress shielding problem could concern fracture healing and result in subsequent fractures due to the significant elastic modulus difference in bulk Ta and human cortical bone[220-221]. Preparing Ta coating is an effective and economical method for the abovementioned causes. The CVD deposited a 30-um thick metallic coating (Ta) on 316L SS, and the findings indicate that the metal coating may offer excellent corrosion protection[222]. According to S.H. Lin's work on

the biomedical Ta coatings assessment of vacuum, plasma-sprayed manufactured Ta coatings significantly improved bioactivity and biocompatibility[223]. In Dulbecco's modified Eagle medium, Ti6Al4V's corrosion resistance, cytocompatibility, and osteogenic activity were all improved by Zhang's deposition of Ta coatings using a combination of α -Ta (tetragonal structure) and β -Ta (BCC structure) phases[224].

In this study, 316L SS is coated with tantalum (Ta) by applying the DC Magnetron sputtering system. Bare and Ta-coated 316L stainless steel was characterized by Optical Microscopy (OM), Optical Emission Spectroscopy (OES), Scanning Electron Microscopy (SEM), Energy Dispersive X-ray Spectroscopy (EDS), and Inductive Coupled Plasma-Mass Spectroscopy (ICP-MS). Bare and Ta-coated 316L stainless steel were investigated by Contact Angle Measurement, Scratch Test, and Biocompatibility studies to determine the candidate biomaterial for higher durability, without internal implant failure and effective performance (especially Ta-coated 316L SS) for orthopedic applications.

6.1 Experimental details

6.1.1 Material and Sample Preparation

Austenitic stainless-steel type 316L was procured from M/s Mishra Dhatu Nigam Limited (MIDHANI), Hyderabad, India, with a dimension of $(472 \times 775 \times 20)$ mm. The received sample was cut into the required dimension of $(20 \times 20 \times 2)$ mm with the help of a table moving Wire Electrical Discharge Machining Machine (WEDM) (Express cut Series-Ex4023C, India). **Table 6.1** shows the chemical composition of the as-received 316L SS alloy used in the experiment. After cutting the 316L SS through WEDM as required dimensions $(20 \times 20 \times$

2 mm), Samples were mirror-polished before deposition of Ta coating using emery paper up to 1600 grit, followed by washing with distilled water and hot air blow-drying. The specimens were then ultrasonically cleaned with acetone for 30 minutes to achieve good adhesion with the coating. Optical microscopy was used to check the substrate constantly to ensure the microstructure of the sample surface.

Table 6.1 The chemical composition of the as-received 316L SS

| Material | C | Mn | S | P | Si | Cr | Ni | Mo |
|----------|------|------|-------|-------|-------|------|------|------|
| 316L SS | 0.03 | 1.39 | 0.005 | 0.003 | 0.015 | 17.5 | 13.6 | 2.27 |

6.1.2 Tantalum deposition

Tantalum thin films were deposited on 316L SS using a Direct Current Magnetron Sputtering (DCMS) technique. It is a thin-film Physical Vapor Deposition (PVD) coating method in which an ionized gas molecule bombards a coating target material, causing atoms to "Sputter" into the plasma; when the particles are vaporized, they condense and produce a thin coating on the substrate to be coated. In the basic sputtering process, energetic ions released in glow discharge plasma bombard the target (cathode) plate. The probability of an ionization electron atom collision increases significantly if electrons are confined in this technique. A magnetron's enhanced ionizing efficiency generates dense plasma in the target region. Consequently, the target is bombarded with more ions, leading to higher sputtering rates and, as an outcome, higher deposition rates on the substrate. Using a DC sputtering machine, the thin film was deposited onto stainless steel 316L with a high purity sputter tantalum target (99.95% Ta) with a diameter of 55.8mm and a thickness of 3.175 mm.

Table 6.2 shows the DC Magnetron sputtering operational parameters for the coating process. Before the deposition operation, the sample was ultrasonically cleaned. Acetone was used in the cleaning process, followed by drying in pure Argon (Ag) gas flow. Each sample's deposition time was 15, 30, and 60 minutes. 316L SS substrates were placed right beneath the target's tracks inside the DC magnetron sputtering. Pre-sputtering was done 15 minutes before each layer deposition technique to clean the surface of the targets and eradicate all impurities and contaminants. A mass flow controller (MFC) was used to control the gas flow. Before the deposition process, the chamber was evacuated to a 5×10^{-4} Pa base pressure.

Table 6.2 DC Magnetron sputtering operational parameters for the coating process

| Parameters | Details |
|--|-----------------------------|
| Target Material | Tantalum (Ta) |
| Magnetron Source | 02 Nos. (50.8 mm each) |
| Working Temperature | $180^{\circ}\text{C} \pm 1$ |
| Voltage | 240-277 V |
| Subtract the holder's distance from the target | 70mm |
| Speed | 7-9 rpm |
| Working Pressure | 5×10^{-1} Pa |
| Base Pressure | 5×10^{-4} Pa |
| Chiller Temperature | $20^{\circ}\text{C} \pm 1$ |
| Gas | Argon (Ar) |

6.1.3 Microstructural Characterization

The 316L SS surface was examined using an Optical Microscope (**OM, Leica Z6 APO**). Scanning Electron Microscopy (**SEM, ZEISS MA 15/18, United Kingdom**) was used to analyze the surface morphology of the 316L SS. The chemical composition of the samples was assessed using Energy Dispersive X-ray Spectrometry (EDS) and Optical Emission Spectroscopy (OES) (**01J0054, Worldwide Analytical Systems AG, Germany**). An Inductively Coupled Plasma Mass Spectrometry (**Agilent 7800 ICP-MS mainframe, Agilent Technologies**) analytical method was used to analyze elements in physiological fluids at trace levels.

Preparation of samples for ICPMS: The weights of samples were determined by weighing on a digital balance (Model No. K-BA 200, K-Roy instruments India) with 0.0001g accuracy; the bare 316L SS have weight 0.686g, 0.803g Ta-coated (15min.), 0.560g Ta-coated (30min.), and 0.797g Ta-coated (60min.) 316L SS. They dissolved in aqua regia (16ml of HCl and 4ml of HNO₃) and then kept in fume hude for complete dissolution in 100ml of the beaker. After complete dissolution (at pH of 2.0), a solution was poured into 10ml of distilled water to achieve ppm after 50X to all the bare and coated samples.

6.1.4 Contact Angle Measurement

Using contact angle measuring equipment [**Drop Shape Analyzer-DSA 25 (Kruss)**], water contact angle measurements were used to determine the wettability of the films' surface. A drop of liquid from a syringe is applied to the surface of the test material using the sessile drop technique. The advancing CA may be determined after the reduction is applied to the material, generally using a goniometer. A goniometer records the drop on the test material, and the data analysis is used to determine the advancing angle at the liquid-solid interface.

6.1.5 Scratch Test

Adhesive coating strength was evaluated by applying the Scratch test (**Scratch Tester TR-101 Ducom**). The standard diamond stylus for scratch testing has a 200 μm radius spherical tip and Rockwell C geometry with a 120° cone. Scratch testing includes sliding a diamond stylus over a sample's surface simultaneously, providing a normal force that is gradually or continuously increased until a critical normal force is achieved. At this moment, a precisely articulated coating failure occurs. The adhesion would then be determined using this force. The progressive vertical force is being used in the test. When a scratch penetrates through the coat, there seems to be a material fracture and force variations that follow. This is considered a critical force.

6.1.6 Biocompatibility Test

All samples with a dimension of $(20 \times 20 \times 2)$ mm were used for the cell culture (Cell Adhesion and Cell Proliferation) investigation. Cells of human bone osteosarcoma named **MG-63** were utilized in this study. The cells were maintained at 37°C in a humidified 5% CO_2 incubator (Galaxy®170 S, Eppendorf, Germany) using Dulbecco's modified Eagle's medium supplemented with 10% fetal bovine serum and 1% penicillin (10 000 U ml^{-1})/streptomycin (10 mg ml^{-1}) (PS).

Cell adhesion and proliferation assessment: The assessment was performed on the bare and Ta-coated 316L SS samples placed in a 35mm petri dish, per the standard procedure. The samples were sterilized by using an autoclave. The autoclaved samples were placed in a 35mm petri dish. MG63 cells were seeded with a density of 1×10^4 on each sample and incubated at 37°C and 5% CO_2 . The sample was cultured till day 14. For staining, media was removed from each petri dish and washed thrice with PBS. The sample was fixed with 4% paraformaldehyde. Further, Triton-X was added for 5 min. To block nonspecific binding, 1%BSA in PBS was added. Finally,

rhodamine-phalloidin was added and incubated for 1h. Then, DAPI (1 μ g/ml) was incubated for 30 min in the dark. The entire experiment was performed in triplicates.

6.2 Results and Discussion

6.2.1 Microstructural Characterization

6.2.1.1 Optical Emission Spectroscopy (OES)

The elemental composition analysis was carried out with the help of the OES. The elements with respect to the atomic weight percentages (average wt %) of bare stainless steel 316L were Fe (64.1), C (0.13), Si (<0.15), Mn (1.39), P (<0.003), S (<0.005), Cr (17.5), Mo (2.27) and Ni (13.6) as shown in **Fig. 6.1**. The peak wavelength identifies the element. The peak area or intensity indicates the amount of the element present in the sample. The analyzer utilizes this data to estimate the sample's elemental composition with verified reference material as the basis for calibration.

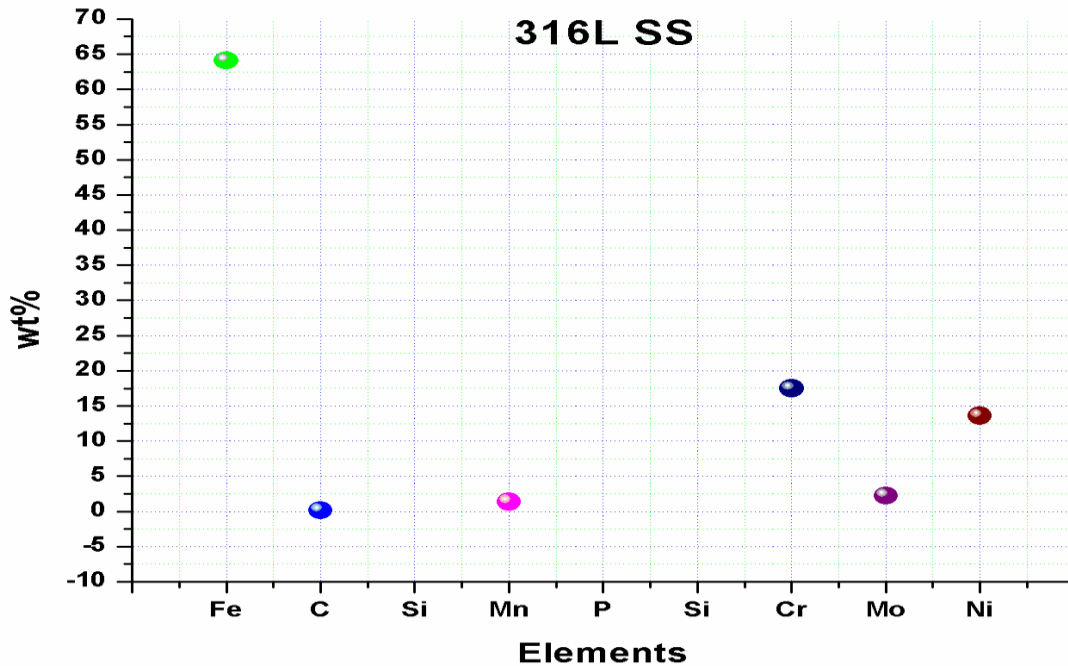


Fig. 6.1 OES results for 316L SS

6.2.1.2 Optical Microscopy (OM)

Fig. 6.2 shows the optical microscopy images at a 50 μ m scale of both Ta-coated and bare 316L SS. **Fig. 6.2(a)** shows the bare surface of 316L SS in which grain boundaries can be seen clearly when the surface is etched with aqua regia, and **Fig. 6.2(b)** shows the Ta-coated 316L SS surface only uniform tantalum coating with no visible grains appears. Coated surfaces were examined in order to check the surface morphology against bare 316L. As per ASTM E3, the surface was polished successively with finer abrasives until the finish was finished so that the material would reflect as much light as possible.

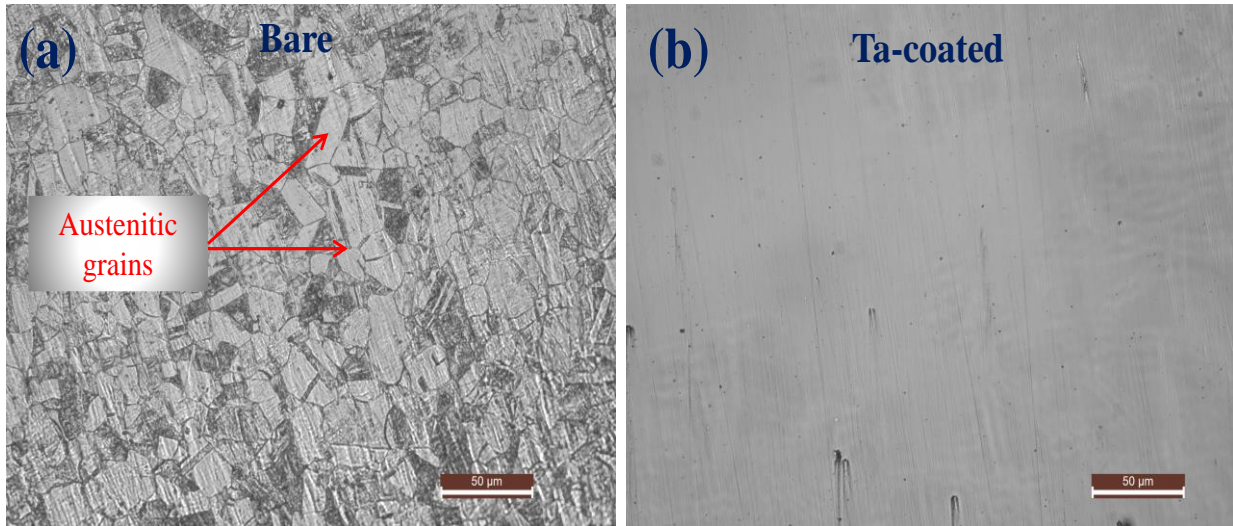


Fig. 6.2 Optical Microscopy images of 316L SS (a) Bare (b) Ta-coated

6.2.1.3 Scanning Electron Microscopy (SEM)

After tantalum coating over 316L SS, the coating thickness is determined by doing a cross-sectional cut and analyzing SEM (Except Bare 316L SS). After three iterations, the average coating thickness data are presented. **Fig. 6.3** presents the SEM image of the cut coating. The lowest average width for a 15 min. deposition was $1.504 \pm 0.019 \mu\text{m}$ for 30 min. deposition, it was 3.809 ± 0.015 and the highest thickness for a 60 min. deposition was $6.083 \pm 0.008 \mu\text{m}$.

The cell adhesion and cell proliferation methods were performed for 1-day, 7-days, and 14-days incubation time to evaluate the cell behaviour. It is found that the 14-day incubation period obtained a maximum number of human osteoblast MG-63 at Ta-coated (coating thickness of $6.089 \mu\text{m}$) 316L SS. Scanning Electron Microscopy results of bare and Ta-coated 316L stainless steel suggest that the human osteoblast MG-63 was well adherent over the coated surface compared to the bare substrate. In vitro investigations that simulate the interaction of bone-forming cells with implant materials frequently use MG-63 cells. The Ta-coated 316L SS does not inhibit

cell adhesion, as seen by the increase in surface covering with the period of time when cells are observed by SEM. After 1, 7 and 14 days of incubation, the MG-63 cells revealed a significant difference in the Ta-coated 316L SS and 316L in terms of cell proliferation.

Thus, it is clear that the Ta-coated 316L SS has no adverse effects on cell proliferation, suggesting that this tantalum-coated stainless steel has the potential to be biocompatible. The ability of an implant's surface to develop apatite is a necessary precondition for long-term and robust bone fixation in orthopaedic surgical applications; a higher implant's capacity to produce apatite promotes the rapid formation of a layer of physiologically active, bone-like apatite on its surface, strengthening bone conductivity[204]. For both coated and uncoated 316L SS samples, the cell viability using the MTT test, following 48 hours, MC3T3-E1 osteoblast cells were used to assess cell viability in both samples due to very robust surface protection that prevented the release of metal ions from the samples, the coated samples' cell viability was greater (95.80%) than that of the uncoated ones (54.72%). The coated samples had higher surface roughness and more cells per unit area. As a result, cells that were linked to the sample coated more rapidly and covered the whole surface [225].

For an implanted material to function effectively inside the human body, it must be biocompatible, which pertains to the way the body endorses it. Each sample's cell count was evaluated to the number of cells detected in the blank group, which was made up of cells cultured in an extract-free medium and calibrated to comprise 100% viable cells. The Ti-6Al-4V group's proliferation rate was considerably lower than that of control groups, while that of the Ta C coating was equivalent to that of control groups, and the Ta C coating had no negative effects on the viability of the cells [201].

SEM observed the adhering MG-63 cells' growth patterns. The cells have diverse biological behaviour on different surfaces (Bare, 15-30 min. Ta-coated 316L SS) after being incubated for 1, 7, and 14 days. The SEM analysis revealed that the Ta coating's structure on a 316L SS substrate appears slightly porous, and no micro-cracks can be dispersed around the structure, as seen in **Fig 6.4**. This is most likely because the deposition process comprised a very rapid cooling rate. The MG-63 cells form a flawless single layer over deposited Ta films, keep their original natural shape, and reflect the usual regular pattern. **Fig. 6.4** shows for the 14 days incubation period, that coated surface had a higher cell density than the untreated 316L. The findings show that these cells and the Ta films are significantly amicable. It is visible that the deposited layer contains granular features at the nanoscale. The deposition parameters, in particular the sputtering pressure and optimized sputtering power, have a significant impact on the film surface characteristics. These considerations mainly affect the residual kinetic energy of the ad atoms and the mean free path of ions to reach the least energy site on the substrate for film development [216]. In comparison to the group control of bare 316L SS, Ta-coated samples showed superior ability to modify and adsorb ions and, as a result, better bioactivity performance. Both Ta-based surfaces displayed Ca/P values after 14 days of immersion in SBF that were close to those of hydroxyapatite (Ca/P 1.67), especially the oxide coating with a value of 1.73. The CP Ti Gr2 surface control exhibits the lowest Ca/P ratio, indicating that the osseointegration procedures need to continue somewhat slowly [217].

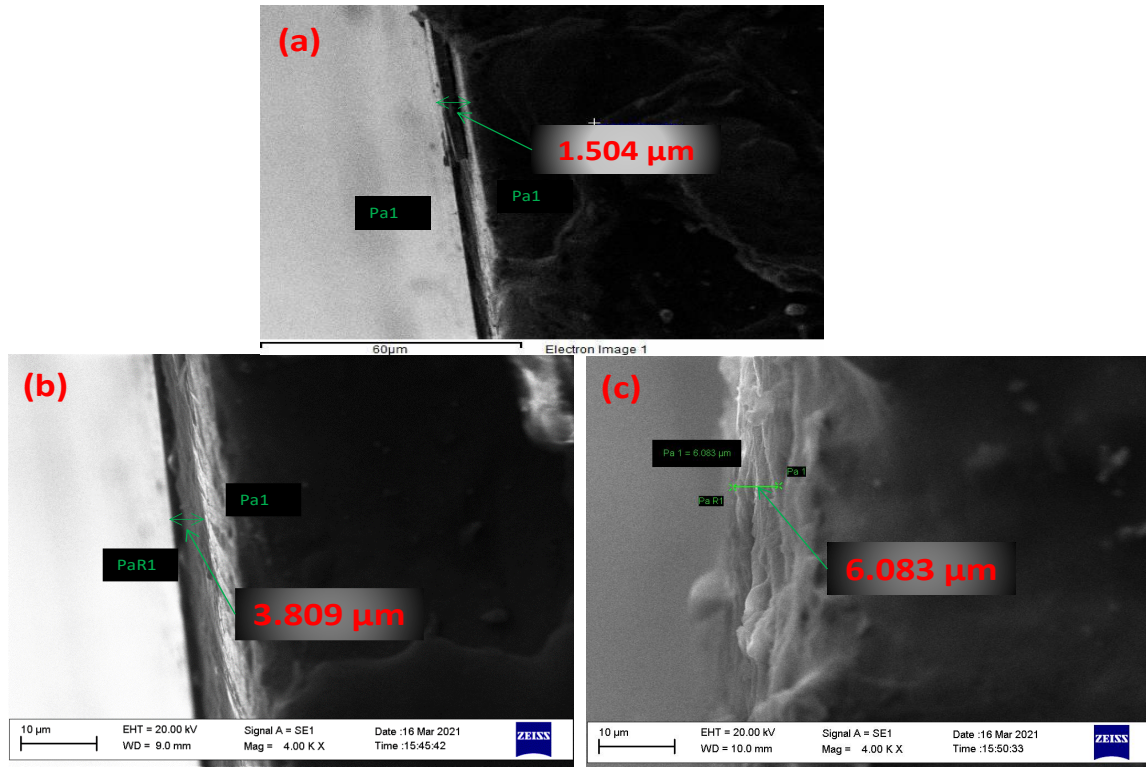


Fig. 6.3 SEM images of cross-section cut coating before the biocompatibility test of Ta-coated 316L SS (a) Ta-coated (15min.) (b) Ta-coated (30min.) (c) Ta-coated (60min.)

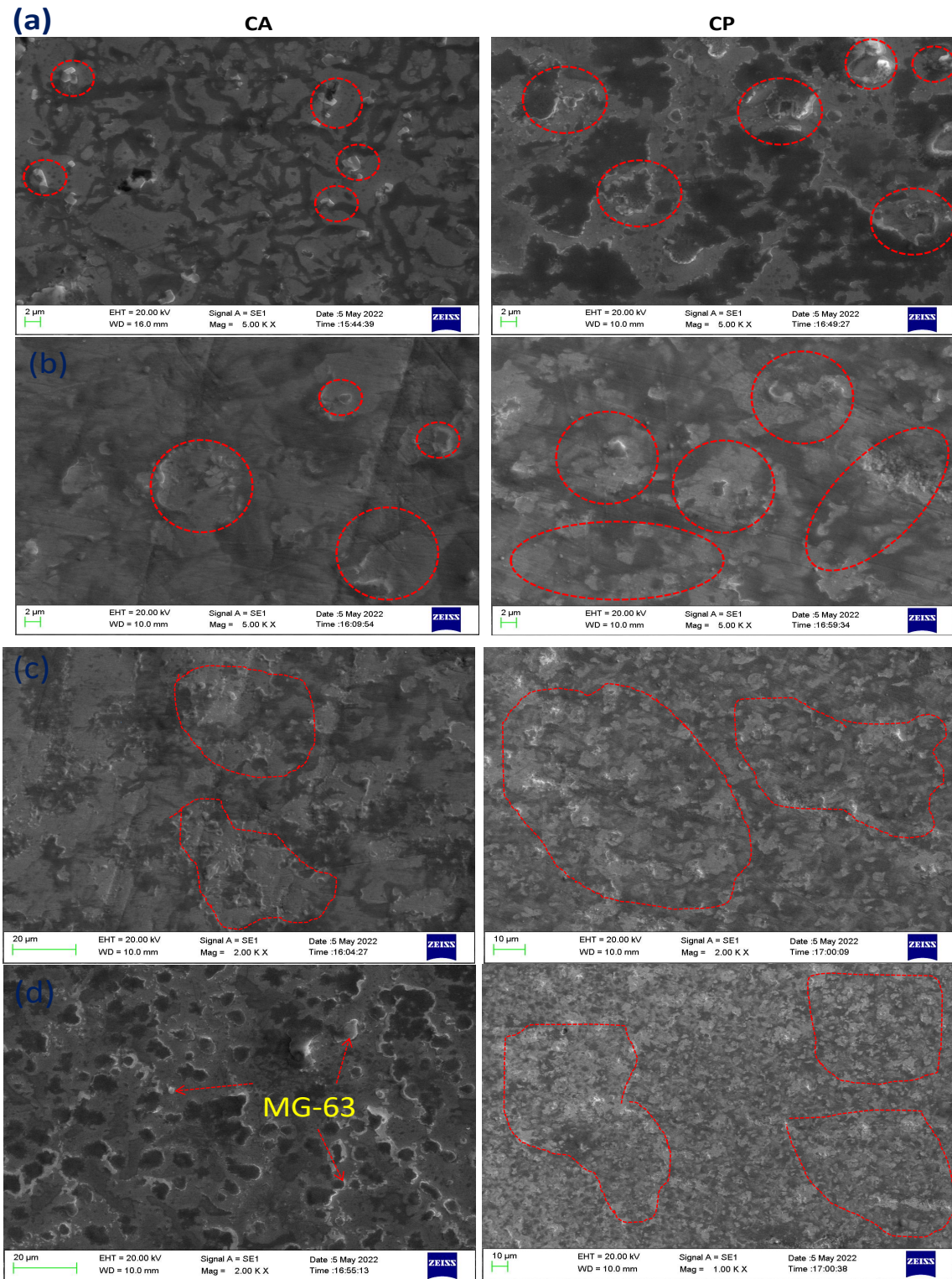


Fig. 6.4 SEM images of MG-63 Osteoblast culture for **1-day** incubation on bare and coated 316L SS (a) Bare (b) Ta-coated 15min., (c) Ta-coated 30min., (d) Ta-coated 60min.

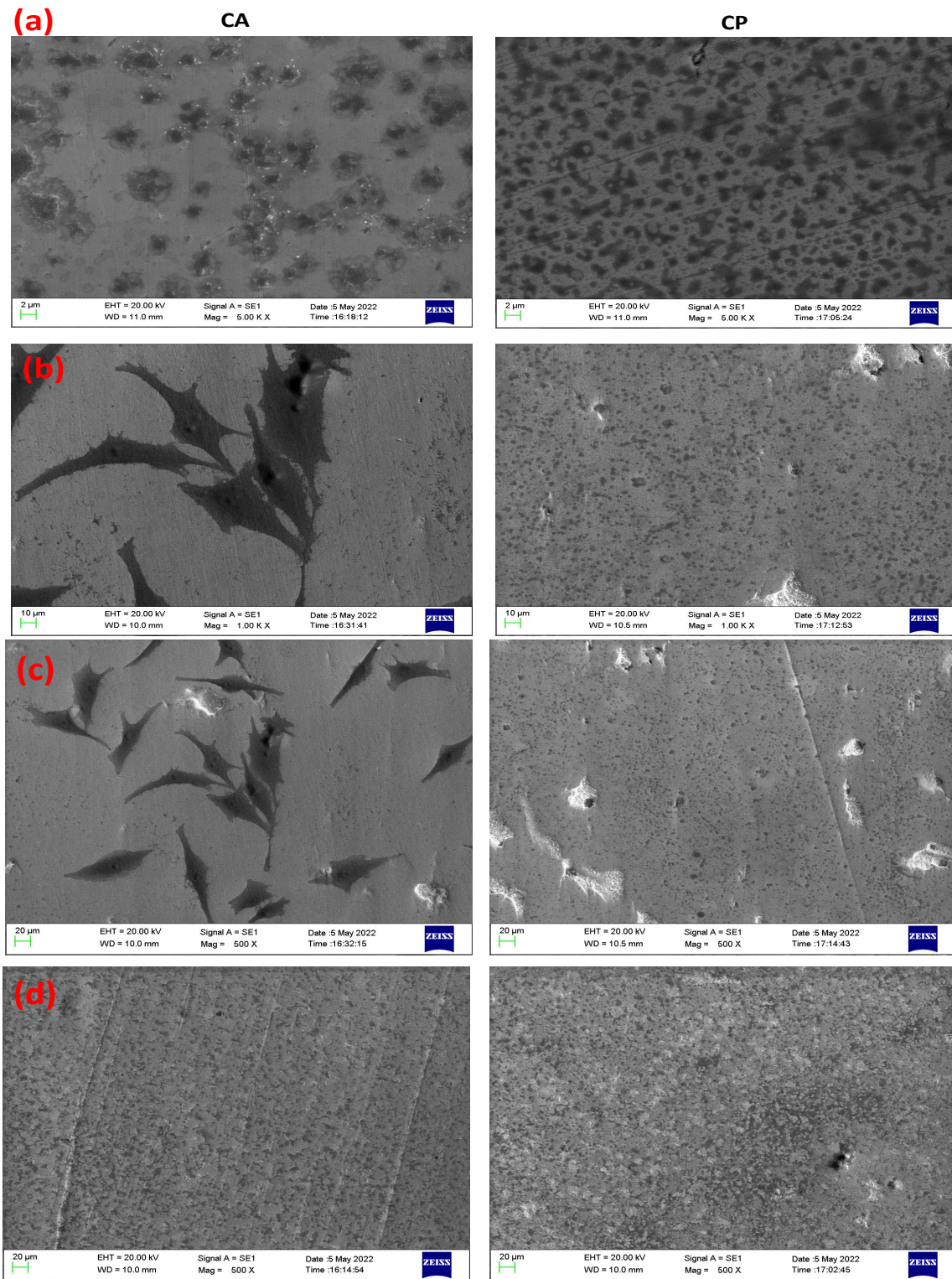


Fig. 6.4(continued) SEM images of MG-63 Osteoblast culture for **07-days** incubation on bare and coated 316L SS (a) Bare (b) Ta-coated 15min., (c) Ta-coated 30min., (d) Ta-coated 60min.

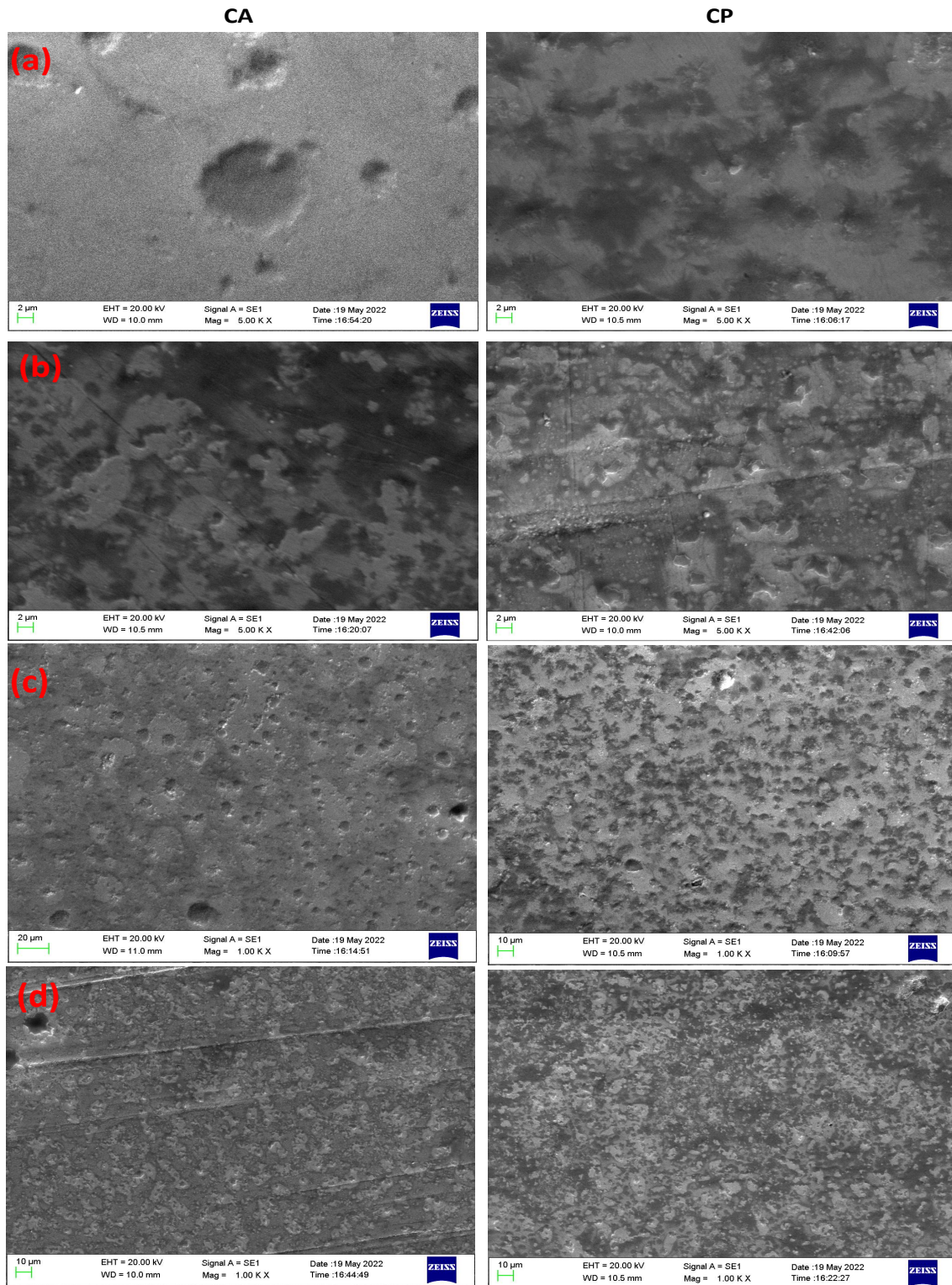


Fig. 6.4(continued) SEM images of MG-63 Osteoblast culture for **14-days** incubation on bare and coated 316L SS (a) Bare (b) Ta-coated 15min., (c) Ta-coated 30min., (d) Ta-coated 60min.

6.2.1.4 Energy Dispersive X-ray Spectrometry (EDS)

A typical Ta coating surface microstructure and the results of an EDS examination after **one day** of cell adhesion and cell proliferation are shown in **Fig. 6.5**. According to the findings of the EDS investigation, Ta occupies the majority (95.33 and 93.33 wt. %) of the coating. The presence of Cr and Ni is higher in cell adhesion compared to cell proliferation. In other words, the magnetron sputtering process prevents the coating surface from oxidizing, which leads to the formation of a high-purity Ta coating. The surface has high roughness values with increasing coating thickness, i.e., $R_a = 14.4 \text{ m}$, significantly greater than the untreated substrate. This is true for coatings of all different thicknesses. Notably, the coating's macro-sized ($5\mu\text{m}$) structure significantly improves biomedical implants' early fixation and ensures prostheses' long-term mechanical stability [26, 27]. The surface of the Ta coating after seven days, as depicted in **Fig. 6.5**, has a slightly finer microstructure than the Ta coating from one day. The EDS data also reveal that the surface contains considerable amounts of Cr, Ni, Mo, and C in addition to Ta. Cell adhesion and cell growth were incubated for 14 days, as shown in **Fig. 6.5**. The results of the EDS analysis revealed that the coated surface shares a significant amount of tantalum over the surface of 316L stainless steel. It is interesting that the C peaks are more invisible than their corresponding peaks for 1 and 7 days of incubation.

Energy dispersive X-ray spectrometry analyses of both the types of samples (bare and Ta-coated) 316L stainless steel were carried out after the biocompatibility test (cell adhesion and cell proliferation for 1 day, 7 days, and 14 days). It is observed that Cr, Ni, Mo, Mn, C, and Fe were present in bare 316L SS. The majority of Ta is observed in coated 316L SS along with all these elements, as presented in **Fig. 6.5**. When Ta-coated samples were subjected to cell adhesion for 01

days, higher wt% of Ta is obtained compared to the cell proliferation. In the cell adhesion and cell proliferation test over the bare 316L SS, element C was absent after the incubation period of 14 days. It indicates that the existence of C is only up to the 07 days of investigations of the Cell adhesion and proliferation tests.

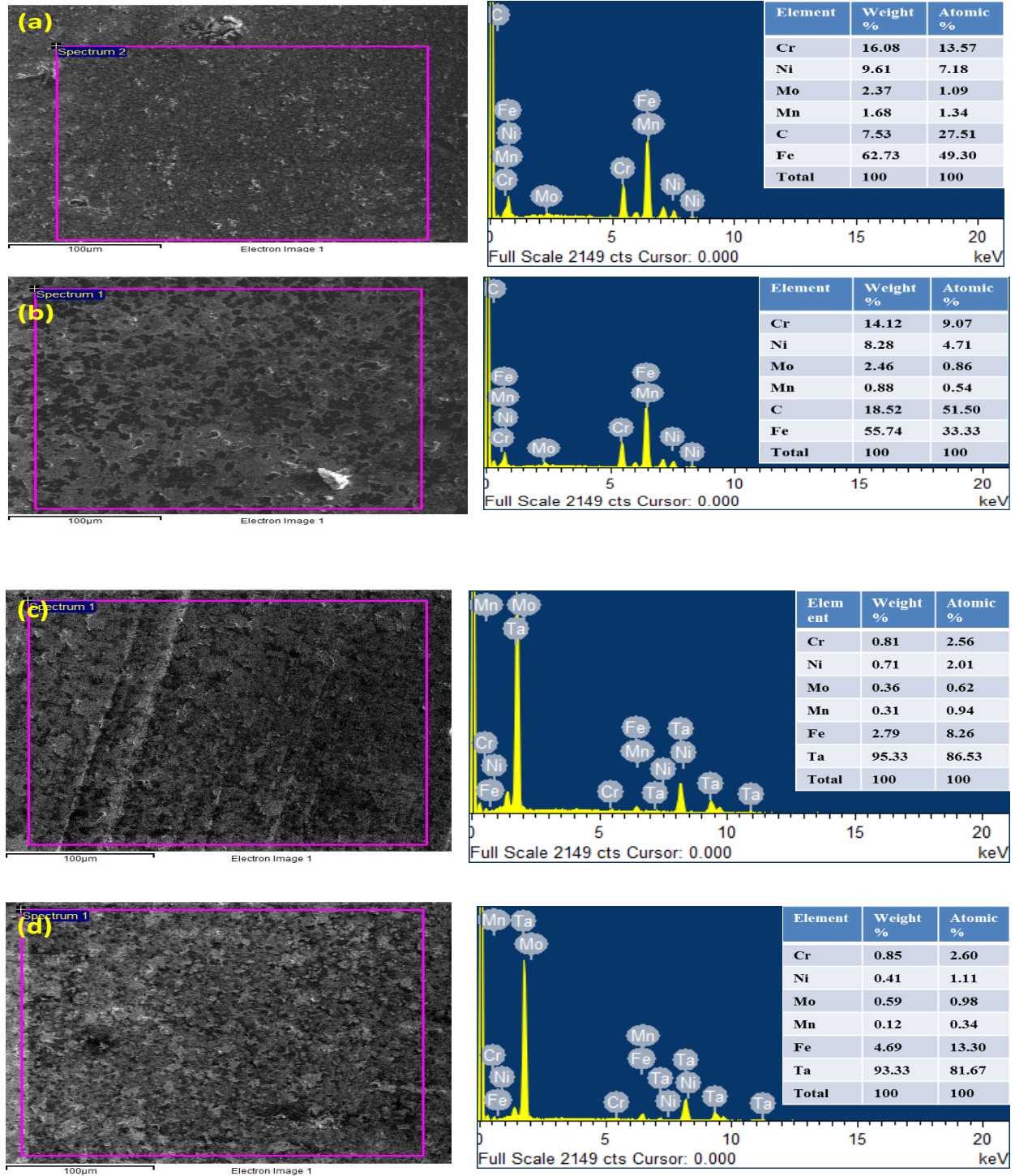


Fig. 6.5 EDS images for **1-day** of bare and Ta-coated 316L SS (a) Bare (cell adhesion) (b) Bare (cell Proliferation) (c) Ta-coated (cell adhesion) (d) Ta-coated (cell Proliferation)

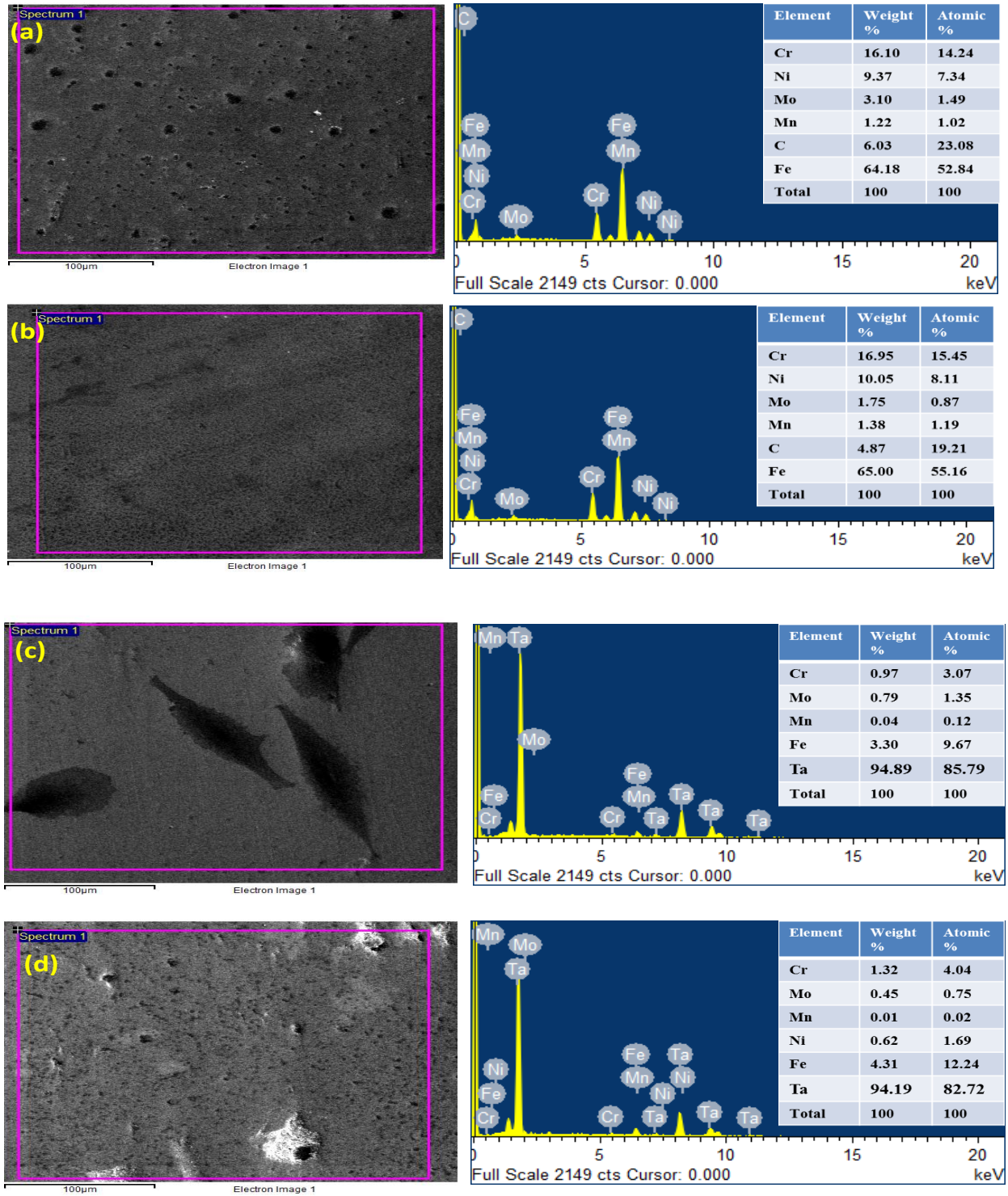


Fig. 6.5(continued) EDS images for 7-days of bare and Ta-coated 316L SS (a) Bare (cell adhesion) (b) Bare (cell Proliferation) (c) Ta-coated (cell adhesion) (d) Ta-coated (cell Proliferation)

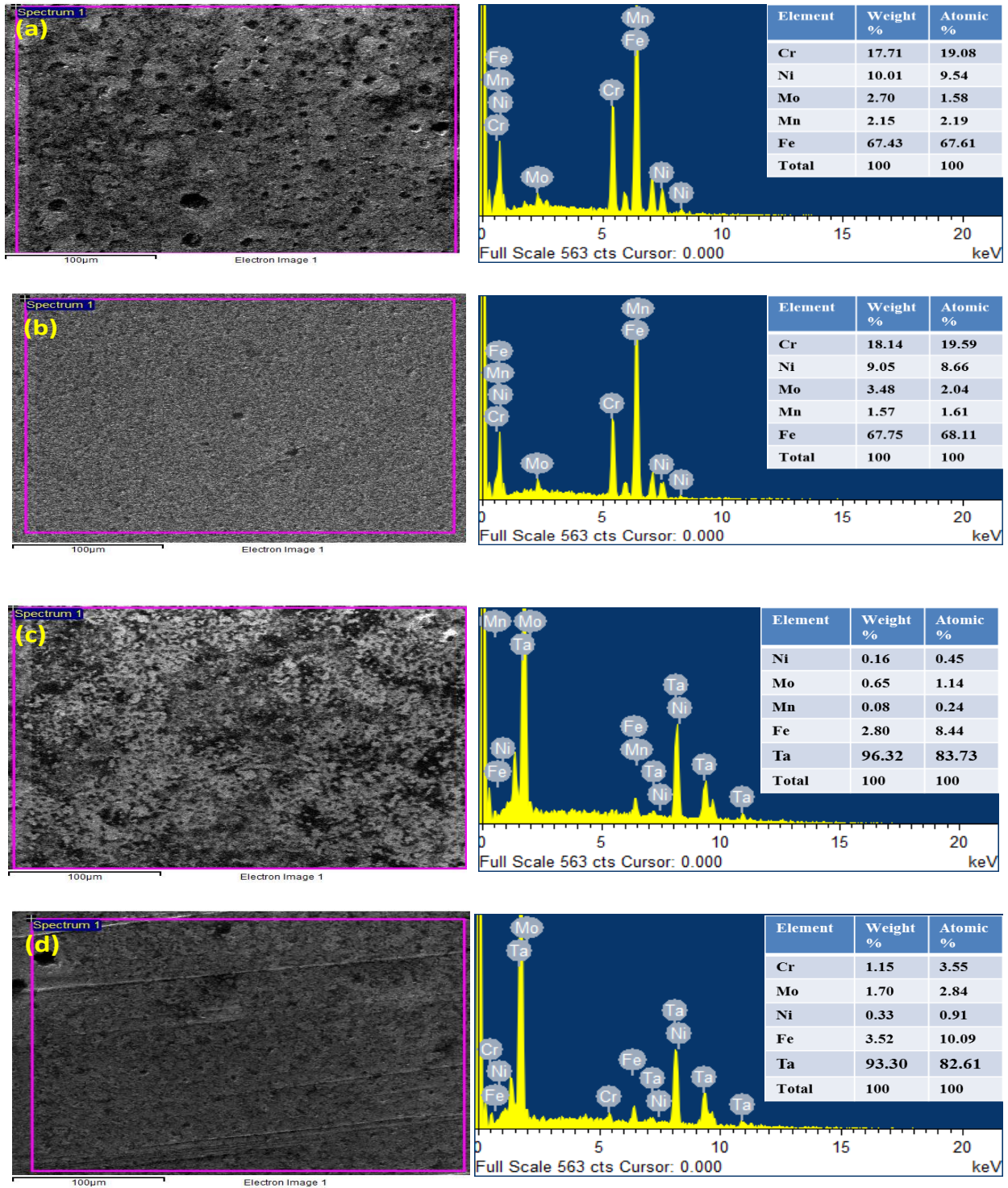


Fig. 6.5(continued) EDS images for **14-days** of bare and Ta-coated 316L SS **(a)** Bare (cell adhesion) **(b)** Bare (cell Proliferation) **(c)** Ta-coated (cell adhesion) **(d)** Ta-coated (cell Proliferation)

6.2.1.5 Inductively Coupled Plasma-Mass Spectrometry (ICP-MS)

Fig. 6.6 Shows the element, concentration and CPS results of various ranges of elements to differentiate the elemental composition of the samples and shows the basic terminology for the concentration (ppm) and CPS against the no. of elements to clearly signify the presence of the Cr, Mn, Ni and Mo which are the major elements in the stainless steel 316L. The Ta-coated samples from 15min. to 60min. coating with the thickness of 1.504 μm , 3.089 μm , and 6.015 μm to improve the concentration of Ta (0.007, 0.009 and 0.098) with respect to the CPS.

A calibration curve may be built using calibration standards with known elemental concentrations in order to translate this data into a concentration value. The term "external calibration" refers to this method. Many different clinical contexts can be useful in the assessment of trace elements in biological specimens. Iodine, manganese, copper, selenium, and zinc are among the necessary elements that are checked for nutrition-related reasons. These substances are crucial for a variety of biological functions, such as oxygen and electron transport, hormone production, and catalysis of biological events. Other elements, including arsenic, cadmium, mercury, and lead, are analysed to determine exposure because it is recognized that they have harmful impacts (frequently via a variety of different mechanisms)[226].

Only primary elements of 316L SS (Cr, Ni, Mo and Mn) and Ta-coated 316L SS (Ta, Cr, Ni, Mo and Mn) were evaluated with the help of ICPMS shown in **Table 6.3**.

Table 6.3 Experimental results of ICPMS of Bare and Ta-coated 316L SS

| Parameters | | | 316L SS | | Ta-coated (15 min.) | | Ta-coated (30min.) | | Ta-coated (60 min.) | |
|-------------|------|-------------|-------------|--------------------------|------------------------|--------------------------|-----------------------|--------------------------|------------------------|--------------------------|
| Elem ent | Mass | Time (s) | CPS | Concent ration (%) | CPS | Concent ration (%) | CPS | Concen tration (%) | CPS | Concen tration (%) |
| Cr | 55 | 0.1000 | 64177335.71 | 19.017 | 85431302.06 | 25.317 | 90655299 | 26.865 | 86955675 | 25.769 |
| Mn | 52 | 0.1000 | 3043333.08 | 1.467 | 3984975.36 | 1.924 | 4235941.10 | 2.046 | 4039632.20 | 1.95 |
| Ni | 60 | 0.1000 | 16117681.43 | 11.996 | 21036890.10 | 15.682 | 22693402 | 16.891 | 21720001 | 16.166 |
| Mo | 95 | 0.1000 | 3818465.57 | 2.353 | 4985069.93 | 3.073 | 5180835 | 3.193 | 4995694.70 | 3.079 |
| Ta | 181 | 0.1000 | - | - | 40076.19 | 0.007 | 16045.38 | 0.009 | 10023.43 | 0.098 |

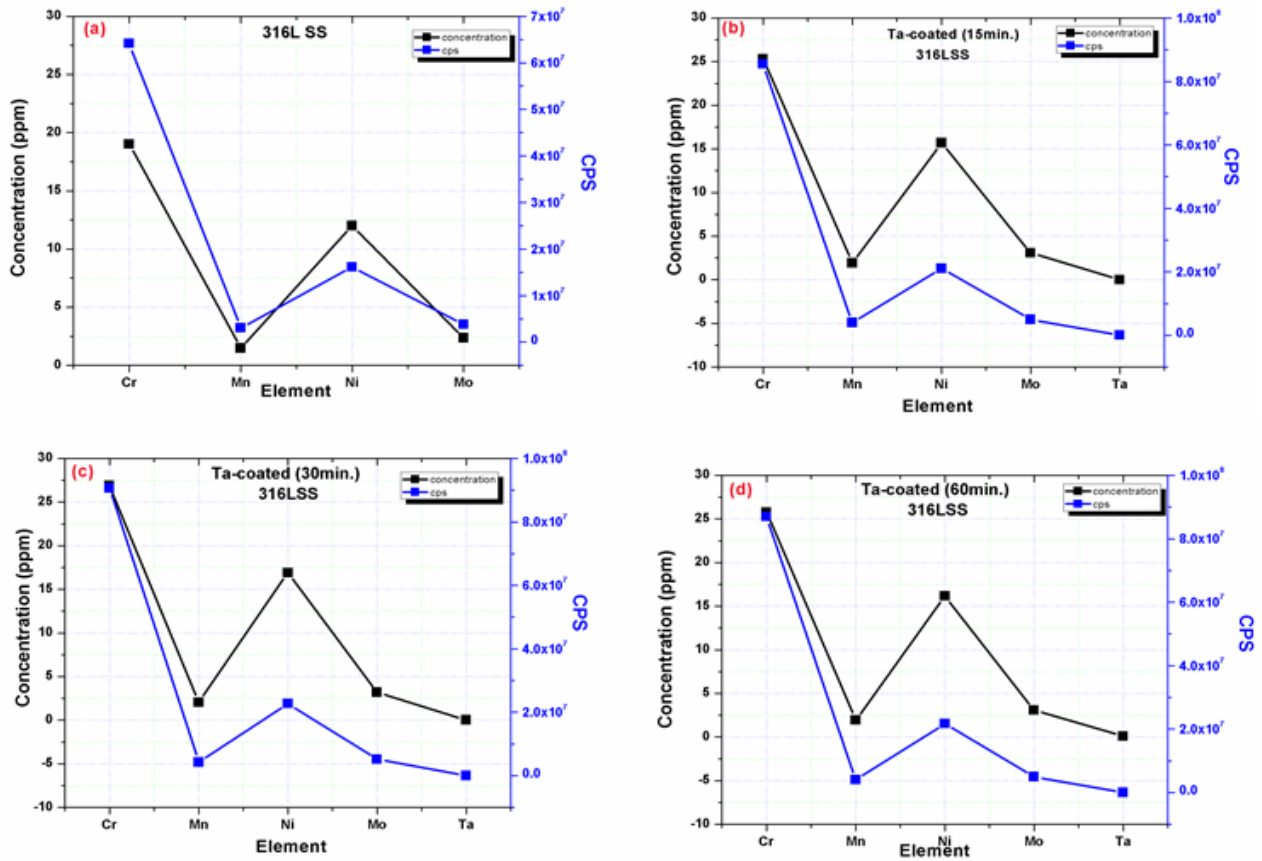


Fig. 6.6 Element, concentration and count per second (CPS) images of bare and Ta-coated 316L SS (a) Bare, (b) Ta-coated (15min.) (c) Ta-coated (30min.), and (d) Ta-coated (60min.)

6.3 Contact Angle Measurement

The Goniometer was used to investigate the contact angle of the bare and Ta-coated 316L SS while maintaining a relative humidity and temperature of 40% and 20°C, respectively. The tests were carried out using a deionized drop mode rate of 2.66 $\mu\text{L/s}$, volume 2 μL . The super-speed digital camera (U4 series 520 frames/second) was used to capture images of the droplet shape on the machined workpiece at intervals of 5s, and an ellipse (Tangent-1) fitting method was employed. Each time a drop of deionized distilled water (about 2 μL) was placed on the sample, a pipette was used to ensure that a drop of deionized distilled water was placed on the sample, as shown in **Fig.**

6.7. For each type of surface treatment, five measurements were performed, and the average value of the static contact angle was calculated as presented in **Table 6.4**. The wettability and surface energy of the Ta films were evaluated using sessile contact angle methods. Compared to hydrophobic surfaces, stronger cell adhesion forces help create hydroxyapatite layers, while surfaces are hydrophilic[227].

Table 6.4 Contact angle measurement values for five iterations of bare and Ta-coated 316L SS

| Sample | Iteration-1 | Iteration-2 | Iteration-3 | Iteration-4 | Iteration-5 | Average (°) |
|-----------------------|-------------|-------------|-------------|-------------|-------------|--------------|
| Bare | 70.90 | 89.40 | 85.30 | 81.40 | 78.50 | 81.10 |
| Ta-coated (15 min) | 71.8 | 64.8 | 76.1 | 65.7 | 74.3 | 70.54 |
| Ta-coated (30 min) | 72.90 | 76.20 | 62.20 | 69.80 | 70.50 | 70.32 |
| Ta-coated (60 min) | 63.50 | 54.40 | 46.90 | 57.70 | 59.90 | 56.50 |

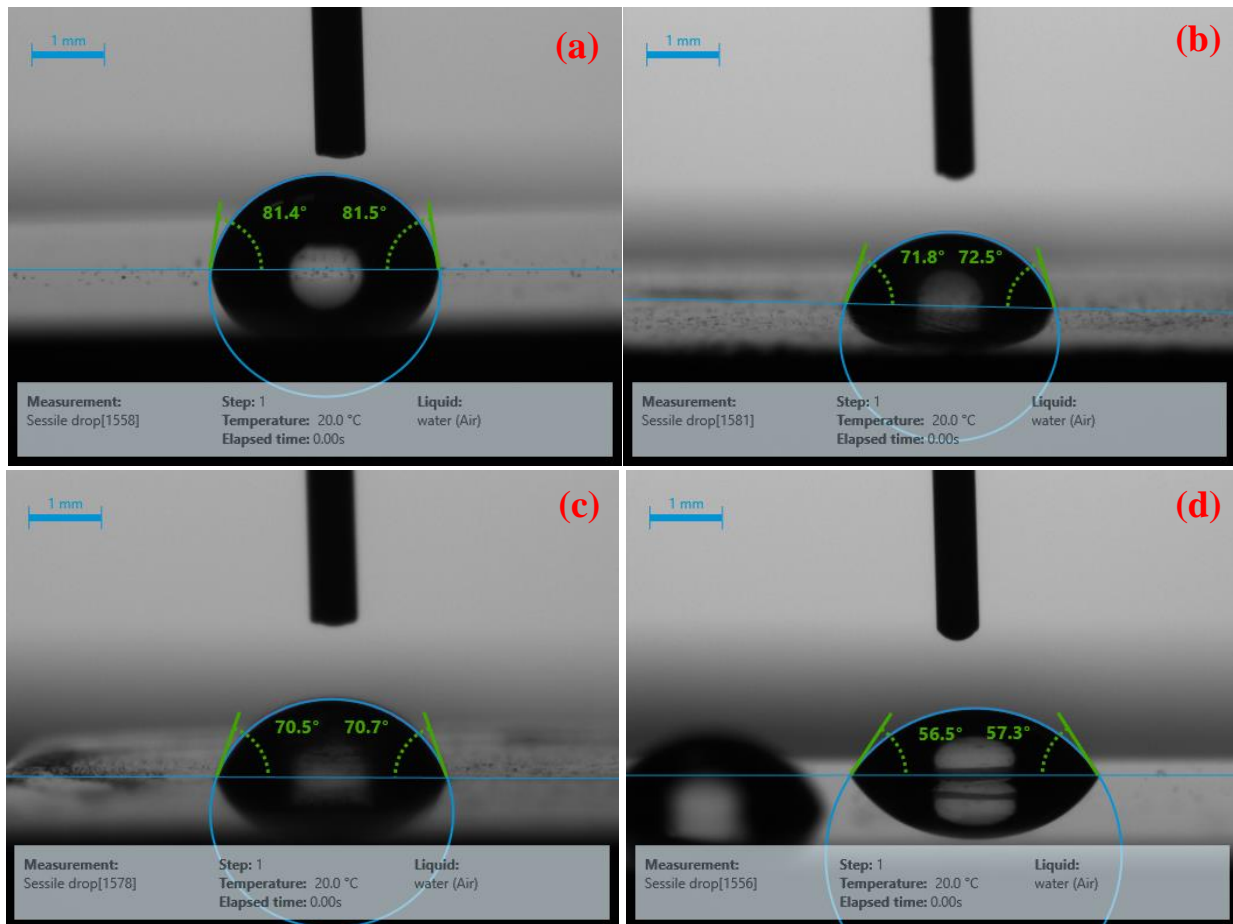


Fig. 6.7 Contact Angle Measurement of 316L SS (a) Bare (b) Ta-coated (15 min) (c) Ta-coated (30 min) (d) Ta-coated (60 min)

The literature sections established that cell adhesion and proliferation are significantly influenced by various factors, including roughness and surface wettability at both the nano and micro levels. Regulating cell adhesion to surfaces is indeed very important for biological studies and diagnosis[228]. In general, the chemical nature of materials and their surface roughness impact their contact angle most [229]. When the contact angle between the surface is less than 90 degrees, according to Wenzel's equation, the contact angle will decrease with increased roughness[230]. Hydrophilic surfaces generally have low fouling and may effectively eliminate cell adhesion or

blood platelet activation, hence improving biocompatibility. Both bacterial and mammalian cell adhesion are anticipated to be reduced if protein fouling is minimized [231].

Hydrophilicity appears to be a key characteristic of temporary medical devices like catheters. The ease with which a catheter can be placed and removed is related to hydrophilicity, which is related to lubricity. Friction between the material and the mucosa can harm the patient and lead to pain[215]. Surface topography has a direct impact on biological reactions at the cellular level, such as cell orientation and migration, as well as their ability to construct structured cytoskeletal structures[215]. When a liquid contacts a solid at an interface, the contact angle represents the angle between the liquid's surface and the outline of the contact surface (lower cos theta). Water contact angle measurement is supposed to be a relatively easy, useful, and sensitive technique for analyzing surface hydrophilicity or hydrophobicity, surface heterogeneity, surface roughness, solid surface energy, liquid surface tension, and line tension[232]. The contact angle reflects a thermodynamic relationship known as the Young equation, which can determine whether a solid's surface is wettable by a liquid, i.e., the interaction between a solid and a liquid surface at the interface. The values of the dispersive energy and polar energy of the Ta films can be obtained by monitoring the contact angles of 5 distinct liquids and using prior surface force values[232]. The angle is related to the interfacial solid-vapour (SV), solid-liquid (SL), and liquid-vapour (LV) free energies (γ) as follows:

$$\gamma_s = \gamma_{sv} + \gamma_v \cos\theta \quad (1)$$

In this study, the roughness of the Ta coatings increases, and the contact angle decreases with time of deposition. Therefore, the increased interaction with the Ta coating may be the origin of the Ta

coating's increased surface roughness and decreased contact angle during 30 and 60 min of deposition.

6.4 Scratch Test

The ASTM [A. International, "Test Method for Measuring Mechanistic Aspects of Scratch/Mar Behavior of Paint Coatings by Nano Scratches" in D 7187-05] standard recommends performing the progressive scratch test on the same specimen at least three times. The test sample is securely held in a chuck mounted on a motorized translation table with a controlled normal load; a stylus is pressed on the surface (F_n). The normal load servo-control ensures that, despite surface waviness, it is precisely maintained at the level needed. While the stylus scratches the surface, the tangential force (F_t) at the contact is measured. **Table 6.5** shows the Scratch test parameters for bare and Ta-coated 316L SS. The ratio (R) of F_t and F_n is the coefficient of friction according to the surface damage threshold. The ratio is increased by the additional component that the energy needed to damage the surface provides to F_t over friction. In step and capture mode, overlapping images of scratch are acquired after a run. They are auto-stitched with each other to form a single image that covers the entire scratch from start to finish. This image has been scaled and placed onto the data graph. When a portion of a graph is selected and enlarged, the image's corresponding length is also zoomed in a synchronized manner. Tagging an image to data makes it easier to see image details at a certain range of activity. The adhesion is then measured using this force. As the average surface roughness increases, the adhesion decreases rapidly.

Table 6.5 Scratch test parameters for bare and Ta-coated 316L SS

| Specimen | Start Load (N) | Finish Load (N) | Stroke length (mm) | Scratch offset (mm) | Scratch Velocity (mm/s) |
|--|----------------|-----------------|--------------------|---------------------|-------------------------|
| Bare, Ta-coated (15min., 30min., and 60min.) | 10 | 50 | 4 | 1.00 | 0.1 |
| | 10 | 50 | 4 | 1.00 | 0.5 |
| | 10 | 50 | 4 | 1.00 | 1.0 |

Fig. 6.8 (a) shows the progressive slow fracture and plugging at higher load occurs with respect to the load. The rate shows the plastic deformation predicted to the adhesive wear phenomena at the bare surface of 316L stainless steel. The critical load (L_c) required to remove the coating from the substrate was ascertained using a scratch track test for the Ta coating. **Fig. 6.8 (b-d)** depicts the critical load of Ta coatings determined from the scratch test at various speeds. It has been discovered that a sample coated at ambient temperature achieves a greater adherence to the substrate. “According to **Fig. 6.10**, which depicts the usual morphology of scratch tracks for bare and Ta-coated surfaces was done at 35 °C, large-scale and continuous flaking is seen on a single side of the scratch channel when fractures spread along the coating-substrate interface”. No cracks or flaking are visible, and the scratch tracks are relatively free of coating debris, smooth and clean, indicating satisfactory adhesion between the substrate and coating. The results demonstrate that under these circumstances, the Ta coating adheres effectively to the substrate. Near the scratch, there are only a few small flaws observable. This observation confirms the belief that coatings have superior adherence to the 316L SS substrate since it is consistent with the L_c results obtained. Based on the scanning electron microscope's investigation of scratches, the explanation for Ta's strong bond between coating and substrate may be because greater rates enable impinging particles

to deposit into the substrate with more energy, resulting in high adhesion strength values between substrate and coating.

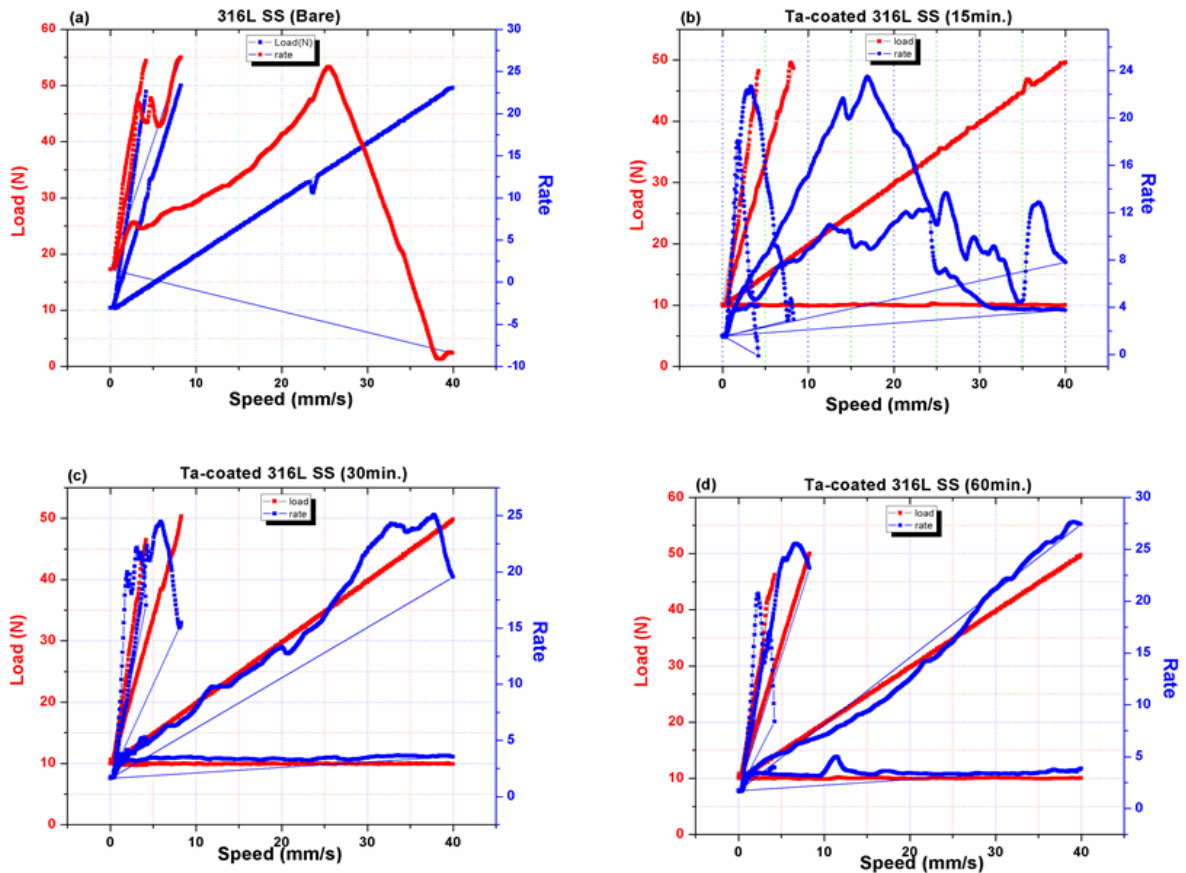


Fig. 6.8 Scratch test surface topography of 316L SS (a) Bare (b) Ta-coated for 15min. (c) Ta-coated for 30min. (d) Ta-coated for 60min.

Fig. 6.9 represents the bench top scanning electron microscopy (BT-SEM) images of scratch test over the bare and Ta-coated 316L stainless steel. The Scratch test was performed at the velocities of 0.1, 0.5, and 1.0 mm/s at load from 10N to 50N and a stroke length of 4mm. Based on the results, it is found that the surface morphology of bare 316L SS is more affected in terms of fracture, ploughing, and plastic deformation, while little changes occur in Ta-coated surfaces (15min to

60min). It is evident that the surface of coated and bare after the scratch test confirms the strong coating adherent to subtract.

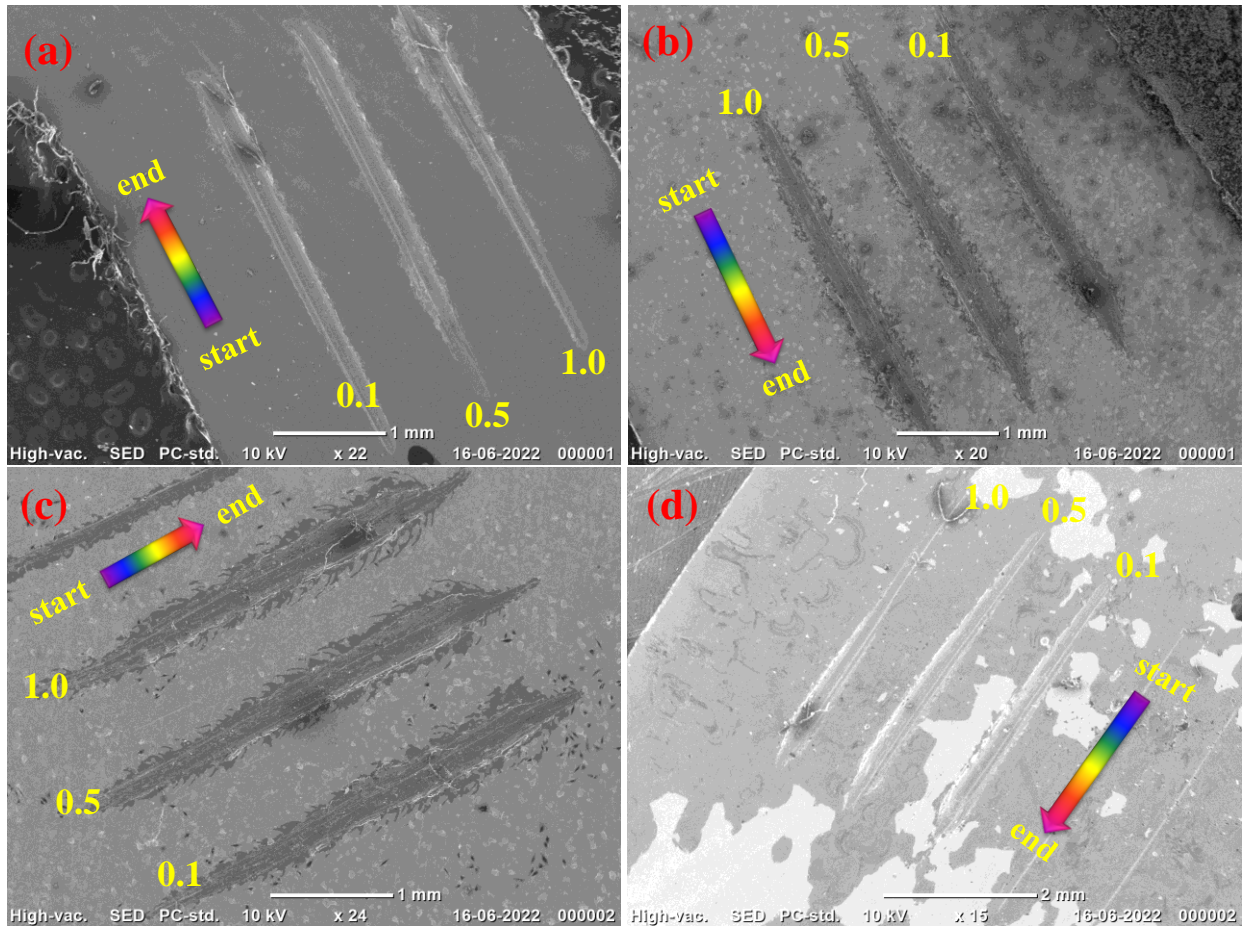


Fig. 6.9 BT-SEM images of scratch test over the bare and Ta-coated 316L SS (a) Bare (b) Ta-coated (15min) (c) Ta-coated (30min) (d) Ta-coated (60min)

Fig. 6.10 shows the 3D topography of scratch test images of bare and Ta-coated 316L SS, in which **Fig. 6.10 (a)** represents the bare surface after the scratch test confirms the plastic deformation and ploughing occurs at a higher load. Plastic deformation with ductile fracture was observed in Ta-coated (15 min) 316L SS, as shown in **Fig. 6.10 (b)**. **Fig. 6.10 (c)** displayed the Ta-coated (30 min) surface, which was found to be a little brittle fracture with sub-surface cracks occurring at higher loads. Compared to the bare surface, the Ta-coated (60 min) shows lower ploughing and

contaminations at a higher load. The coating adhesion is found to be more effective on the same surface.

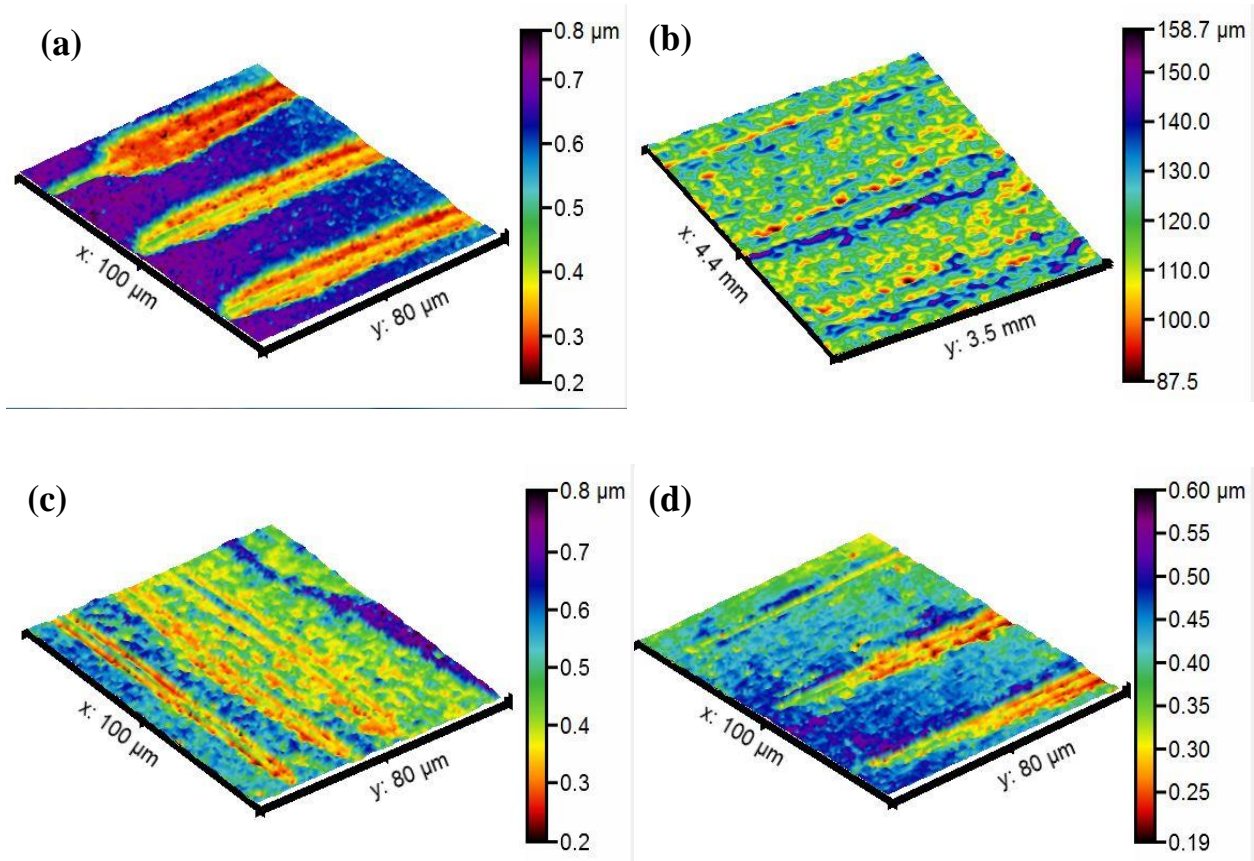


Fig. 6.10 3D topography of scratch test images 316L SS (a) Bare (b) Ta-coated (15min) (c) Ta-coated (30min) (d) Ta-coated (60min)

The thickness of the coating plays a vital role in improving the adhesion strength of 316L stainless steel, as thickness increases with increasing adhesion strength, as depicted in **Fig. 6.11**. Based on the experimental observation, it is found that bare 316L has $4\mu\text{N}$ adhesion strength, while Ta-coated 15, 30, and 60 min. samples obtained $7\mu\text{N}$, $17\mu\text{N}$, and $23\mu\text{N}$ adhesion strength respectively.

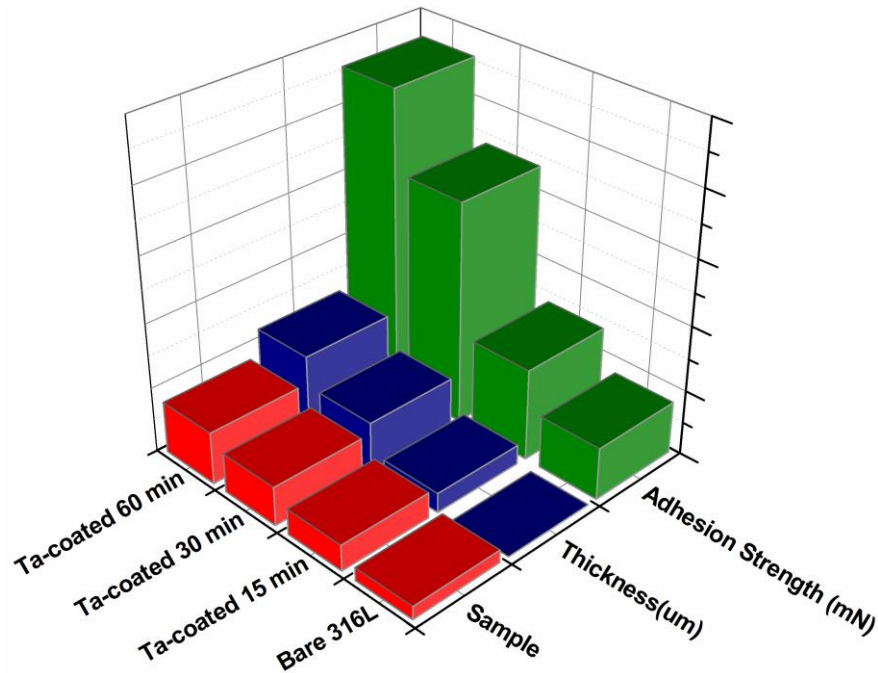


Fig. 6.11 Thickness and adhesion strength diagram

6.5 Biocompatibility

Cell adhesion and cell proliferation were performed for 40 samples of Bare and Ta-coated 316L SS, shown in **Table 6.6**. Finally, 24 samples got accurate results with the Cell adhesion and cell proliferation test based on characterization results, photographic images of bare and Ta-coated 316L SS for biocompatibility test presented in Fig. 6.12.

According to the characterisation results, the Ta coatings applied for 15, 30, and 60 min had enhanced biocompatibility in the PBS solution. As a result, their cytocompatibility, including toxicity and proliferation, has been further studied. Fusiform cells are distributed evenly over all specimens in the low-magnification images, with no evident signs of direct contact. Compared to 316L SS, the relative density of adhered osteoblasts on Ta-coated samples increases, indicating their superior ability to promote cell adhesion[224]. The spreading ability of osteoblasts on the

316L SS and Ta coatings reveals no substantial difference in the enlarged images. High magnification images, however, make it clear that osteoblasts adhere better easily to Ta coatings than to 316L SS, confirming the positive interaction between osteoblasts and Ta coatings.

Table 6.6 Sample plan (Bare and Ta-coated) for biocompatibility test

| Duration (days) | Sample | Cell Adhesion | Cell Proliferation | Cell toxicity & proliferation assessment using MTT assay |
|-----------------|--|---------------|--------------------|--|
| 1 | Bare = 1 15min. = 1 30min. = 1 60min. = 1 | 04 | 04 | 04 |
| 7 | Bare = 2 15min. = 2 30min. = 2 60min. = 2 | 08 | 08 | 08 |
| 14 | Bare = 2 15min. = 2 30min. = 2 60min. = 2 | 08 | 08 | 08 |
| Total | | 20 | 20 | 20 |

The Ta coating for 60 min has more adherent cells and higher spreading ability than the other Ta-coated specimens, suggesting that it is more conducive to osteoblasts' physiological activity. The quantitative proliferation of osteoblasts cultured for 1, 7, and 14 days on 316L SS and Ta-coated specimens. On a 1-day, there was no statistically significant difference between the groups.

Because 316L SS and Ta are both suitable biomedical materials, the amount of harmful ions that dissolve from 316L SS is so tiny that it cannot significantly affect cell growth[232]. After 1, 7, and 14 days of culture, particularly for 14 days, there is a considerable improvement in the differentiation between osteoblasts on 316L SS and Ta coatings.



Fig. 6.12 Photographic images of bare and Ta-coated 316L SS for biocompatibility test

The Ta coating applied for 60 minutes has a more significant absorbance than the Ta coating applied for 30 minutes or the 316L SS, indicating that it has the maximum capacity for osteoblast proliferation. Because of its excellent corrosion resistance and biocompatibility, metallic implants like austenitic stainless steel have been utilized extensively in medicine[233]. However, few researchers have examined the ideal conditions for Ag/Ag Ta₂O₅ produced at various annealing temperatures regarding antibacterial activity and biocompatibility[234]. This reduction in cell growth may result from the cell's response to the different environments of the material surface, which is distinctive from that on the culture flask's particle surface. From the literature [8], the proliferation rate of MG-63 cells, particularly on day 14 in Ag/Ag-Ta₂O₅ at 400 °C, is 42% (p = 0.01) and 33% (p=0.01) in 316L SS as compared to day 1. The experimental results of this study at the same temperature of both the bare and coated samples on day 14 were found to be better (51.42%, p=0.01 for Ta-coated and 41.03%, p= 0.01 for 316L SS) compared to day 1. Process efficiency might be greatly increased by a layer of film that adheres firmly and can cover surfaces from contamination and disorder[205]. Excessive metal ions are released into the surroundings due to the many types of deterioration that occur in implants. This has serious adverse effects on the patient's health that have been implanted[235].

Therefore, surface modifications are needed to fix the problem while improving the surface's roughness and biocompatibility qualities. **Fig. 6.13** displays the fluorescence microscopic images of the MG-63 human bone osteosarcoma cells cultivated on the bare and coated surfaces of 316L Stainless steel. In all samples, the cell coverage increases substantially as the culture time increases, indicating a progressive expansion in cell size with time. Cells are observed proliferating over time for both specimens. After 14 days of culture, cells on the surfaces of tantalum-coated

surfaces are revealed to be widely spread and dispersed. For both (coated and uncoated) stainless steels, there was satisfactory cell coverage across the whole surface area. However, a noticeable difference in the cell coverage may be seen after 7 days of cell culture. It is extremely complicated to differentiate between the cell coverage after 1 day of exposure because of nuclei clustering in both cases. Biocompatibility effect on Ta-coated (thickness 6.083 μm) 316L stainless steel obtaining the significant osteoblast spreading over the surface confirmed by SEM, also fluorescent images depicted the excellent presence up to 14 days of the incubation period to human osteoblast MG-63. The activity of the cell growth was identical on both types of surfaces. However, on the Ta-coated 316L SS, cell proliferation was enhanced. The fluorescent microscopy images of osteoblast MG-63 in **Fig. 6.13 (a-d)** depicted the Rodamine Phalloidin (Red) and 4', 6 diamino-2-phenylindole (Blue) with merged images of day-1, day-7, and day-14. The cell coverage on the Ta-coated surface was gradually increased against the bare surface, indicating higher proliferation of the tantalum-coated surface.

It is observed manually based on SEM images of (5.0 K x magnification and took the average value of three images) and based on software (image J), analysis was done of fluorescent images resulted that the % of Human cell (MG-63) viability increases with increasing the time on highest in Ta-coated (60 min) and least in the bare 316L SS as depicted in **Fig. 6.14**.

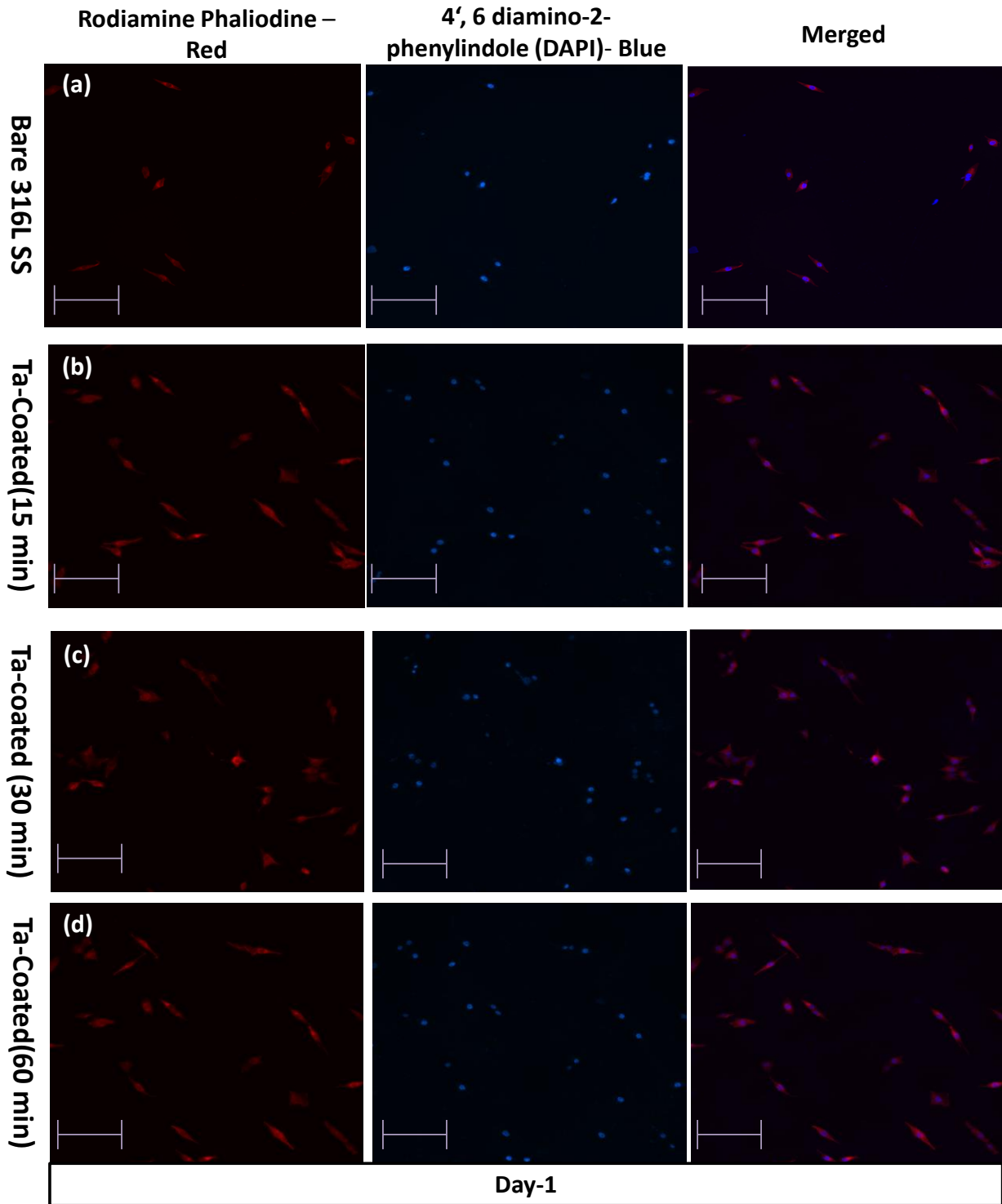


Fig. 6.13 Fluorescent microscopy images of Osteoblast (MG-63) over 316L stainless steel (a) Bare surfaces (b-d) Ta-coated surfaces.

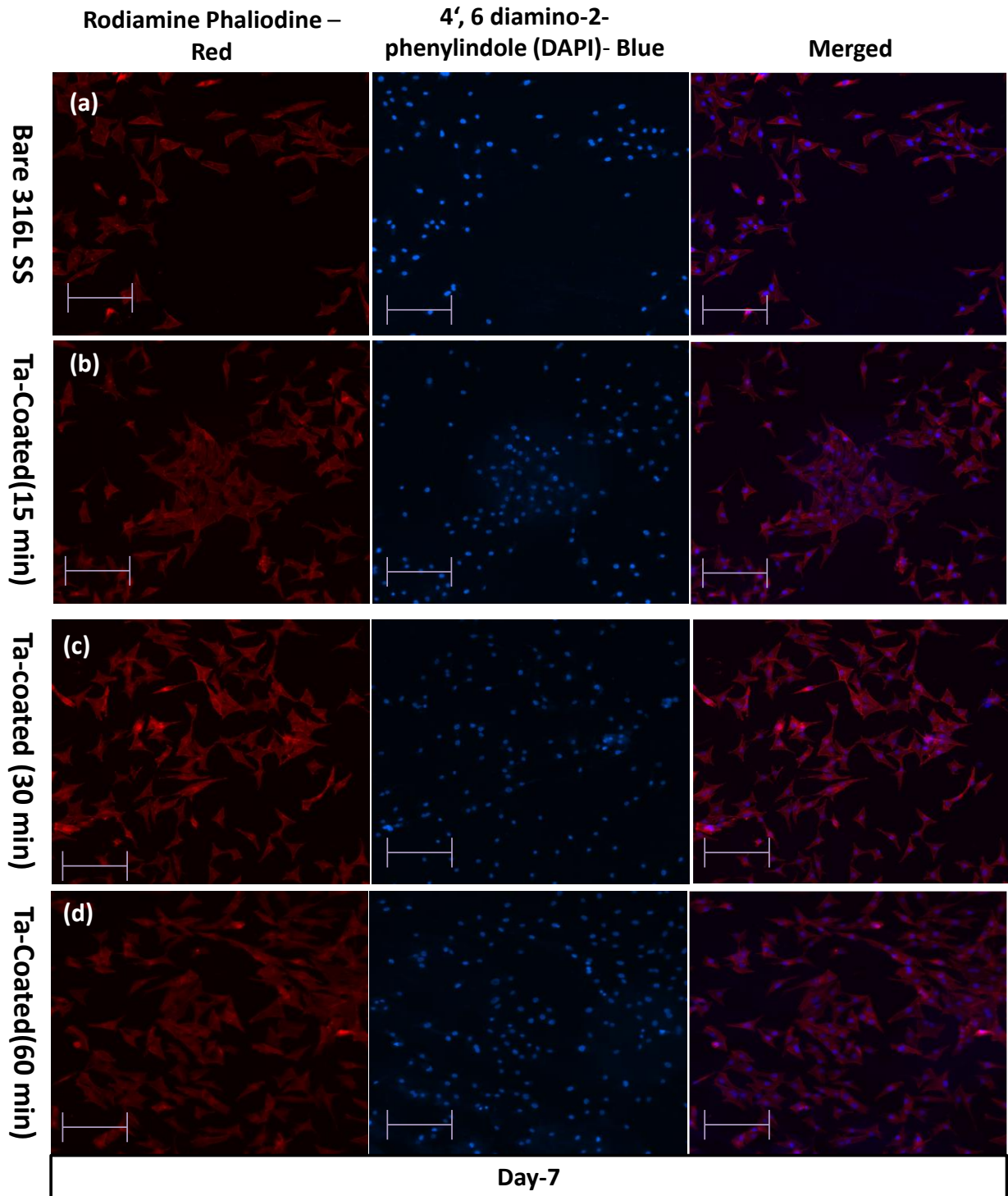


Fig. 6.13(Continued) Fluorescent microscopy images of Osteoblast (MG-63) over 316L stainless steel (a) Bare surfaces (b-d) Ta-coated surfaces.

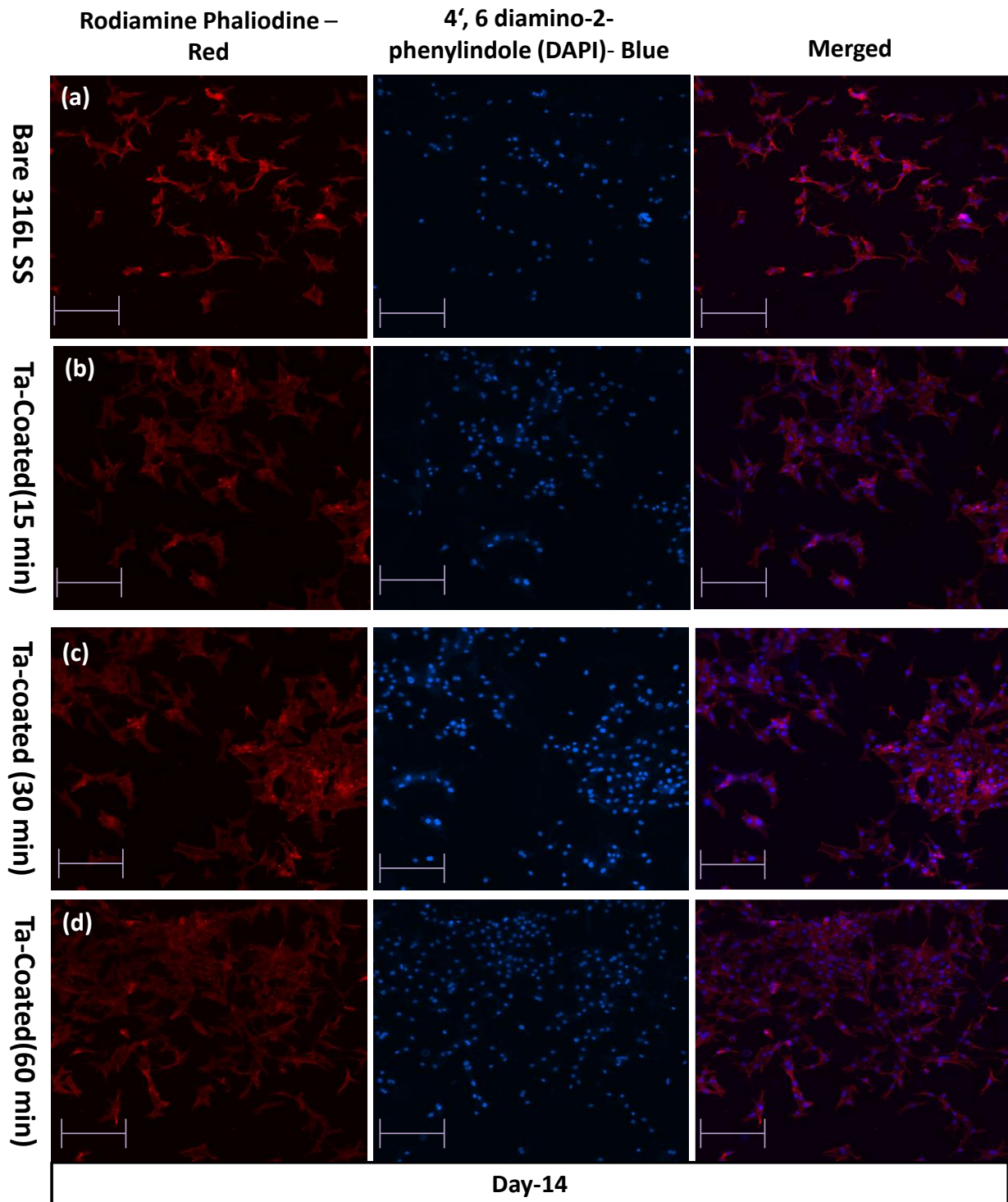


Fig. 6.13(Continued) Fluorescent microscopy images of Osteoblast (MG-63) over 316L stainless steel (a) Bare surfaces (b-d) Ta-coated surfaces.

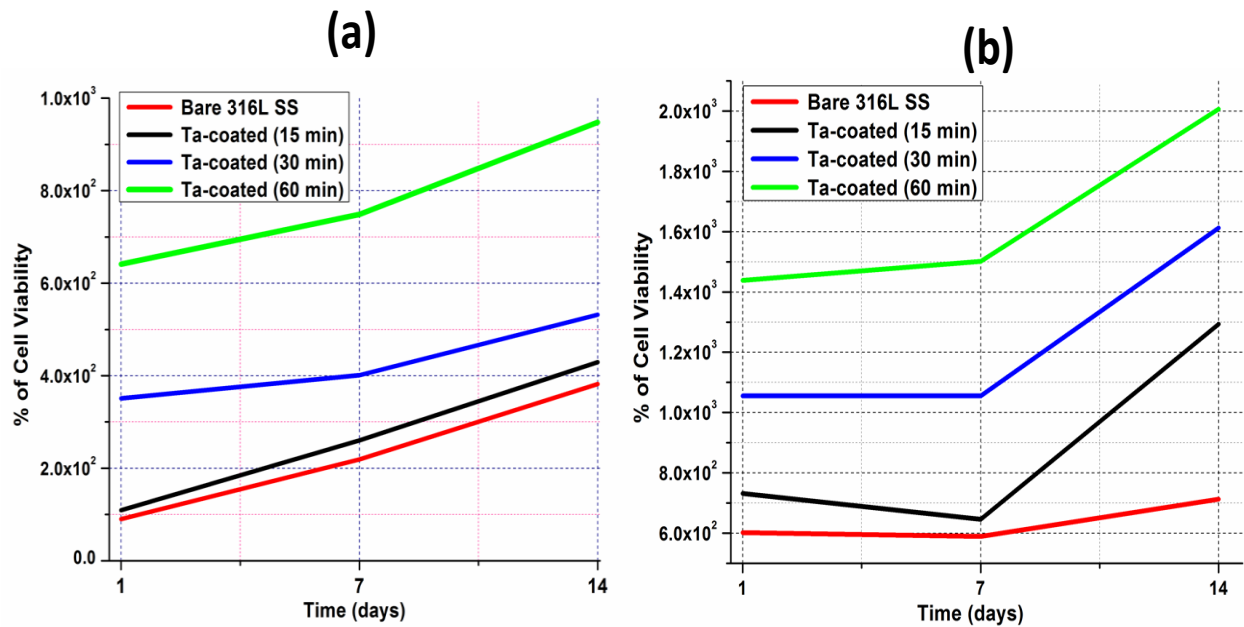


Fig. 6.14 Cell viability and Time image of bare and Ta-coated 316L SS (a) SEM-based analysis (b) Software (Image J) based analysis

6.6 Conclusion

In this study, tantalum coatings formed on 316L stainless steel have been successfully formed using a DC magnetron sputtering system for orthopaedic applications. Furthermore, work has been performed on whether the process parameters influence the modified surface responses. A hydrophilic and uniform thin coating of 1.0504 μm , 3.809 μm , and 6.083 μm , after 15, 30, and 60 min. of coating, respectively, have been found, which has improved the biocompatibility. More than 70% of alive cells and a few dead cells are obtained for the Ta-coated specimen, which ensures improved cell viability, cell proliferation, and biocompatibility. The tantalum coating is preferable to the bare 316L SS for the adhesion and proliferation of MG-63 cells, which reflects its higher biocompatibility, as seen in the in vitro cell-culture investigations. The Ta-coated (60 min) 316L SS demonstrated a significantly greater capacity to promote the formation of an apatite layer that mimicked bone, suggesting that Ta coating can enhance the bioactivity of 316L stainless steel. Hence, the studied Ta-coated 316L SS could improve the lifetime of an implant and can be used for bone applications. These results indicated the applied Ta-coated 316L stainless steel as a promising candidate for 316L stainless steel modification for clinical applications in the body.